We are IntechOpen, the world's leading publisher of Open Access books Built by scientists, for scientists

4,800
Open access books available

122,000
International authors and editors

135M
Downloads

Our authors are among the

154
Countries delivered to

TOP 1%
most cited scientists

12.2%
Contributors from top 500 universities

CLARIVATE ANALYTICS BOOK CITATION INDEX INDEXED

WEB OF SCIENCE™

Selection of our books indexed in the Book Citation Index in Web of Science™ Core Collection (BKCI)

Interested in publishing with us?
Contact book.department@intechopen.com

Numbers displayed above are based on latest data collected.
For more information visit www.intechopen.com

18

Understanding the Vanadium Redox Flow Batteries

Christian Blanc and Alfred Rufer
Laboratoire d'Electronique Industrielle, Ecole Polytechnique Federale de Lausanne
Switzerland

1. Introduction

Vanadium redox flow batteries (VRB) are large stationary electricity storage systems with many potential applications in a deregulated and decentralized network. Flow batteries (FB) store chemical energy and generate electricity by a redox reaction between vanadium ions dissolved in the electrolytes. FB are essentially comprised of two key elements (Fig. 1): the cell stacks, where chemical energy is converted to electricity in a reversible process, and the tanks of electrolytes where energy is stored.

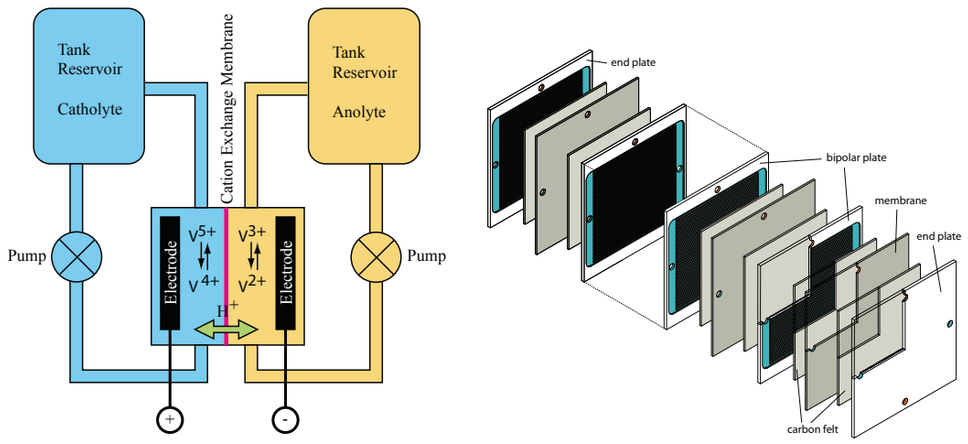

(a) (b)

Fig. 1. (a) The schematics of the vanadium redox flow battery. (b) View of the different components composing a VRB stack. The surfaces in contact with the catholyte are coloured in blue and in orange for the anolyte.

The most significant feature of the FB is maybe the modularity of their power (kW) and energy (kWh) ratings which are independent of each other. In fact, the power is defined by the size and number of cells whereas the energetic capacity is set by the amount of electrolyte stored in the reservoirs. Hence, FB can be optimized for either energy and/or power delivery.
Over the past 30 years, several redox couples have been investigated (Bartolozzi, 1989): zinc bromine, polysulfide bromide, cerium zinc, all vanadium, etc. Among them, VRB has the best chance to be widely adopted, thanks to its very competitive cost, its simplicity and because it contains no toxic materials.

In order to enhance the VRB performance, the system behaviour along with its interactions with the different subsystems, typically between the stack and its auxiliaries (i.e. electrolyte circulation and electrolyte state of charge), and the electrical system it is being connected to, have to be understood and appropriately modeled. Obviously, modeling a VRB is a strongly multidisciplinary task based on electrochemistry and fluid mechanics. New control strategies, based on the knowledge of the VRB operating principles provided by the model, are proposed to enhance the overall performance of the battery.

2. Electrochemistry of the vanadium redox batteries

Batteries are devices that store chemical energy and generate electricity by a reduction-oxidation (redox) reaction: i.e. a transformation of matter by electrons transfer. VRB differ from conventional batteries in two ways: 1) the reaction occurs between two electrolytes, rather than between an electrolyte and an electrode, therefore no electro-deposition or loss in electroactive substances takes place when the battery is repeatedly cycled. 2) The electrolytes are stored in external tanks and circulated through the stack (see Fig. 1). The electrochemical reactions occur at the VRB core: the cells. These cells are always composed of *a bipolar or end plate - carbon felt - membrane - carbon felt - bipolar or end plates*; they are then piled up to form a stack as illustrated in Fig. 1.
In the VRB, two simultaneous reactions occur on both sides of the membrane as illustrated in Fig. 2. During the discharge, electrons are removed from the anolyte and transferred through the external circuit to the catholyte. The flow of electrons is reversed during the charge, the reduction is now taking place in the anolyte and the oxidation in the catholyte.

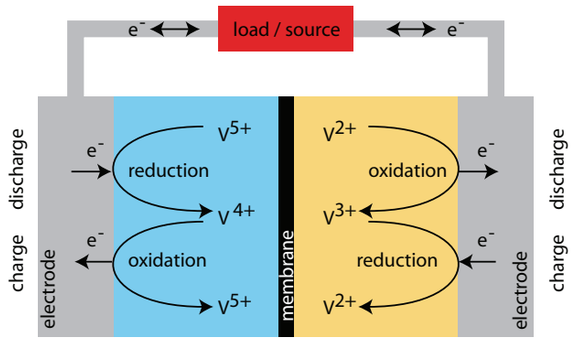

Fig. 2. VRB redox reaction during the charge and discharge

The VRB exploits the ability of vanadium to exist in 4 different oxidation states; the vanadium ions V^{4+} and V^{5+} are in fact vanadium oxide ions (respectively VO^{2+} and VO_2^+). Thus, the VRB chemical equations become (Sum & Skyllas-Kazacos, 1985; Sum et al., 1985):

$$\begin{gathered} VO_2^+ + 2H^+ + e^- \rightleftarrows VO^{2+} + H_2O \\ V^{2+} \rightleftarrows V^{3+} + e^- \\ \hline V^{2+} + VO_2^+ + 2H^+ \rightleftarrows VO^{2+} + V^{3+} + H_2O \end{gathered} \tag{1}$$

where the water (H_2O) and protons (H^+) are required in the cathodic reaction to maintain the charge balance and the stoichiometry.

2.1 Equilibrium potential

The stack voltage U_{stack} depends on the equilibrium voltage U_{eq} and on the internal losses U_{loss}; the equilibrium conditions are met when no current is flowing through the stack. In that case, there is no internal loss and U_{stack} equals U_{eq}; otherwise, the internal losses modify U_{stack}. The internal losses[1] U_{loss} will be discussed in section 3.3. Hence U_{stack} is given by:

$$U_{stack}(t) = U_{eq}(t) - U_{loss}(t) \ [V] \tag{2}$$

The equilibrium voltage U_{eq} corresponds to the sum of the equilibrium potential E of the individual cells composing the stack. This potential is given by the Nernst equation and depends on the vanadium species concentrations and on the protons concentrations (Blanc, 2009):

$$E = E^{\ominus'} + \frac{RT}{F} \ln \left\{ \left(\frac{c_{VO_2^+} \cdot c_{H^+}^2}{c_{VO^{2+}}} \right) \left(\frac{c_{V^{2+}}}{c_{V^{3+}}} \right) \right\} \quad [V] \tag{3}$$

where R is the gas constant, T the temperature, F the Faraday constant, c_i the concentration of the species i and $E^{\ominus'}$ the formal potential. If we assume that the product/ratio of the activity coefficients is equal to 1, the formal potential $E^{\ominus'}$, an experimental value often not available, can be replaced by the standard potential $E^{\ominus}$.

2.1.1 Standard potential from the thermodynamics

The standard potential $E^{\ominus}$ is an ideal state where the battery is at standard conditions: vanadium species at a concentration of 1 M, all activity coefficients γ_i equal to one and a temperature of 25°C . The standard potential is an important parameter in the Nernst equation because it expresses the reaction potential at standard conditions; the second term in the Nernst equation is an expression of the deviation from these standard conditions. Together, they determine the equilibrium cell voltage under any conditions.

The standard potential $E^{\ominus}$ can be found from thermodynamical principles, namely the Gibbs free enthalpy ΔG and the conservation of energy, and empirical parameters found in electrochemical tables. We introduce here the standard Gibbs free enthalpy of reaction $\Delta G^{\ominus}$ which represents the change of free energy that accompanies the formation of 1 M of a substance from its component elements at their standard states: 25°C , 100 kPa and 1 M (Van herle, 2002):

$$\Delta G^{\ominus} = \Delta H_r^{\ominus} - T\Delta S_r^{\ominus} \qquad [kJ/mol] \tag{4}$$

where the standard reaction enthalpy $\Delta H_r^{\ominus}$ is the difference of molar formation enthalpies between the products $\Delta H_{f,product}^{\ominus}$ and the reagents $\Delta H_{f,reagent}^{\ominus}$:

$$\Delta H_r^{\ominus} = \sum_{products} \Delta H_{f,product}^{\ominus} - \sum_{reagents} \Delta H_{f,reagent}^{\ominus} \qquad [kJ/mol] \tag{5}$$

and the standard reaction entropy $\Delta S_r^{\ominus}$ is the difference of molar formation entropies between the products $S_{f,product}^{\ominus}$ and the reagents $S_{f,reagent}^{\ominus}$:

$$\Delta S_r^{\ominus} = \sum_{products} S_{f,product}^{\ominus} - \sum_{reagents} S_{f,reagent}^{\ominus} \qquad [J/mol \cdot K] \tag{6}$$

[1]Note that the sign of U_{loss} depends on the operating mode (charge or discharge).

Then, when we introduce the thermodynamical data from Tab. 1 into (5), the standard reaction enthalpy $\Delta H_r^{\ominus}$ of the VRB reaction (1) becomes:

$$\begin{aligned}\Delta H_r^{\ominus} &= \Delta H_{f,VO^{2+}}^{\ominus} + \Delta H_{f,V^{3+}}^{\ominus} + \Delta H_{f,H_2O}^{\ominus} \\ &\quad - \Delta H_{f,V^{2+}}^{\ominus} - \Delta H_{f,VO_2^+}^{\ominus} - 2\Delta H_{f,H^+}^{\ominus} \\ &= -155.6\ kJ/mol\end{aligned} \tag{7}$$

and similarly, the standard reaction entropy $\Delta S_r^{\ominus}$ is obtained when these thermodynamical data are introduced into (6):

$$\begin{aligned}\Delta S_r^{\ominus} &= S_{f,VO^{2+}}^{\ominus} + S_{f,V^{3+}}^{\ominus} + S_{f,H_2O}^{\ominus} \\ &\quad - S_{f,V^{2+}}^{\ominus} - S_{f,VO_2^+}^{\ominus} - 2S_{f,H^+}^{\ominus} \\ &= -121.7\ J/mol \cdot K\end{aligned} \tag{8}$$

Formula	State	$\Delta H_f^{\ominus}\ [kJ/mol]$	$\Delta G_f^{\ominus}\ [kJ/mol]$	$S_f^{\ominus}\ [J/mol \cdot K]$
V^{2+}	aq	(-226)	-218	(-130)
V^{3+}	aq	(-259)	-251.3	(-230)
VO^{2+}	aq	-486.6	-446.4	-133.9
VO_2^+	aq	-649.8	-587.0	-42.3
H_2O	aq	-285.8	-237.2	69.9
H^+	aq	0	0	0

Table 1. Thermodynamical data for some vanadium compounds at 298.15 K. Values in parentheses are estimated (Van herle, 2002; Bard et al., 1985).

The conservation of energy relates the change in free energy resulting from the transfer of n moles of electrons to the difference of potential E:

$$\Delta G = -nFE \qquad [J/mol] \tag{9}$$

Therefore, we obtain the standard potential $E^{\ominus}$ when we introduce $\Delta G^{\ominus}$ (4) with the values of the standard reaction enthalpy (7) and entropy (8) into the reformulated (9):

$$E^{\ominus} = -\frac{\Delta G^{\ominus}}{nF} = -\frac{\Delta H_r^{\ominus} - T\Delta S_r^{\ominus}}{nF} \qquad [V] \tag{10}$$

So, we have determined from the thermodynamical principles that the standard potential $E^{\ominus}$ is 1.23 V at 25°C .
The characteristic curve of the equilibrium potential E is illustrated in Fig. 3 for a single cell as a function of the state of charge SoC. We can also observe the relation between E, SoC and the protons and vanadium concentrations.

	Salt	Charge	Discharge	Electrolyte
V^{2+}	VSO_4	↑	↓	Anolyte
V^{3+}	$0.5\ V_2(SO_4)_3$	↓	↑	Anolyte
V^{4+} or VO^{2+}	$VOSO_4$	↓	↑	Catholyte
V^{5+} or VO_2^+	$0.5\ (VO_2)_2SO_4$	↑	↓	Catholyte

Table 2. The different vanadium ions with their corresponding salt, their concentration variation during the charge and discharge of the VRB, and the electrolyte where they are dissolved.

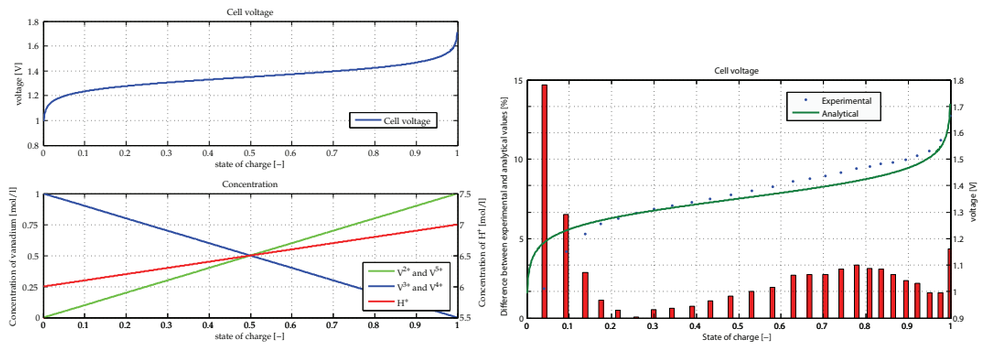

(a) (b)

Fig. 3. (a) Top: Cell voltage versus the state of charge at 25°C. Bottom: Protons H^+ and vanadium concentrations. (b) Comparison between the Nernst equation (3) and the experimental data published in (Heintz & Illenberger, 1998). The red bars represent the difference between the analytical and experimental data.

3. Electrochemical model

The main electrochemical relations governing the equilibrium voltage where introduced in the previous section. In order to have an electrochemical model of the VRB, it is now necessary to describe how the vanadium concentrations vary during the battery operation.

3.1 Concentration of vanadium ions

We see clearly from (1) that during the redox reactions, the vanadium ions are transformed and that some protons H^+ are either produced or consumed. Therefore, the ion concentrations must change in the electrolyte to reflect these transformations which depend on how the battery is operated.

For example, when the battery is charged, V^{2+} and VO_2^+ are produced and their concentrations increase; and V^{3+} and VO^{2+} are consumed and thus their concentrations diminish. This process is reversed when the battery is discharged. Tab. 2 summarizes the direction of the change for each species.

3.1.1 Electron exchange rate

Obviously, the concentration changes are proportional to the reaction rate; and from (1) we also know that an electron is involved each time a redox reaction occurs. Therefore, the concentration changes are also proportional to the electrical current. Thus, the pace of the concentration variation is set by the electrical current flowing through the cell:

$$Q_c = n_{e^-} e = \int i(t)dt \qquad [\mathrm{C}] \tag{11}$$

where Q_c is the charge, i the current, t the time, n_{e^-} the number of electrons and e the elementary charge. Therefore, the number of electrons n_{e^-} involved for a given current[2] is:

$$n_{e^-} = \frac{1}{eN_A} \int i(t)dt \qquad [mol] \tag{12}$$

where N_A is the Avogadro number. Then (12) leads to the definition of a molar flowrate of electrons $\dot{N}_{e^-}$:

$$\dot{N}_{e^-}(t) = \frac{1}{eN_A} i(t) \qquad [mol/s] \tag{13}$$

Physically, an electron is released by the oxidation of a vanadium ion, travels through the electrodes and is captured by the reduction of another vanadium ion in the opposite half-cell. In the case of a stack composed of N_{cell} cells, the electrons travel through the bipolar electrode to the adjacent cell (Fig. 4). Thus, for one electron flowing through the external electrical circuit, N_{cell} redox reactions have occurred. Therefore, the total molar flowrate of electrons $\dot{N}_{e^-_{tot}}$ for a stack is obtained by multiplying (13) by the number of cells:

$$\dot{N}_{e^-_{tot}}(t) = \frac{N_{cell}}{eN_A} i(t) = \frac{N_{cell}}{F} i(t) \qquad [mol/s] \tag{14}$$

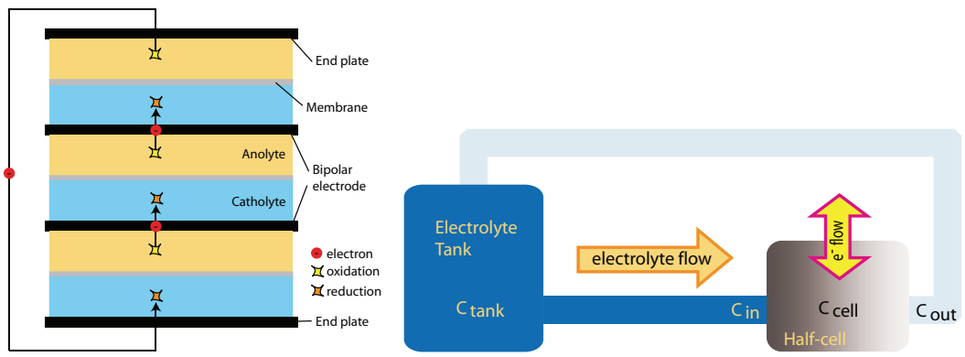

(a) (b)

Fig. 4. (a) Illustration of the redox reactions required to produce a one electron flow in a 3 elements stack during the discharge. When the battery is charged, the flow and the reactions are inverted. (b) Illustration of the hydraulic circuit (half cell) where the concentrations are shown.

[2]By convention, the current is positive during the VRB discharge in order to have a positive power delivered by the battery.

3.1.2 Input, output and average concentrations of vanadium ions

We know now that the vanadium concentrations change within the cells when the battery is operating. Therefore, the concentrations are not uniformly distributed through the electrolyte circuit (Fig. 4). Indeed, four concentrations are located in the VRB: the tank concentration c_{tank}, the concentration at the cell input c_{in}, the concentration inside the cell c_{cell} and the concentration at the cell output c_{out}.

Usually, the size of the reservoir is large compared to the electrolyte flowrate; thus the change in concentrations due to the flow of *used* electrolyte is so small that the tank concentrations are considered homogeneous. And therefore, the input concentrations c_{in} correspond exactly to c_{tank}.

The tank concentration c_{tank} reflects the past history of the battery; indeed the change in c_{tank} is proportional to the quantity of vanadium that has been transformed in the stack: this value corresponds to the quantity of electrons involves in the reaction. Therefore, c_{tank} is defined by the initial ion concentrations $c_{tank_i}^{initial}$, the size of the reservoir V_{tank} and the total molar flowrate of electrons $\dot{N}_{e_{tot}^-}$:

$$\begin{aligned} c_{in_i}(t) = c_{tank_i}(t) &= c_{tank_i}^{initial} + \frac{1}{V_{tank}} \int b \dot{N}_{e_{tot}^-}(t) dt \\ &= c_{tank_i}^{initial} + \frac{1}{V_{tank}} \int \frac{b}{F} i(t) dt \qquad [mol/l] \end{aligned} \tag{15}$$

where b is a sign factor that reflects the direction of the reaction in accordance with Tab. 2:

$$b = \begin{cases} -1 \text{ for } V^{2+} \text{ and } V^{5+} \text{ ions} \\ 1 \text{ for } V^{3+} \text{ and } V^{4+} \text{ ions} \end{cases} \qquad [-] \tag{16}$$

The description of the output concentration c_{out} is difficult because it depends on the electrolyte flowrate Q, the length of the electrolyte circuit and on the current i that the electrolyte encounters during the cell crossing. Since the distribution of the vanadium ions inside the cell is unknown, we consider that the model has no memory and reacts instantly to a change in the operating conditions. In that case, c_{out} is related to the electrons molar flowrate $\dot{N}_{e_{tot}^-}$, the electrolyte flowrate Q and on the input concentration c_{in}:

$$c_{out_i}(t) = c_{in_i}(t) + b \frac{\dot{N}_{e_{tot}^-}(t)}{Q(t)} = c_{in_i}(t) + \frac{b N_{cell}}{F} \frac{i(t)}{Q(t)} \qquad [mol/l] \tag{17}$$

where: c_i = concentration of the different vanadium ions [mol/l]
$Q(t)$ = flowrate of the electrolyte [l/s]

For a quasi steady state, where the current and the flowrate are almost constant, the model predicts accurately the output concentrations. Unfortunately, it is not able to predict the transient behaviour when the system encounters extreme conditions such as the combination of a low flowrate, few active species and sudden current change. But when these conditions are avoided, (17) offers a very good insight of the battery behaviour.

We still have to establish the most important concentration: the concentration inside the cell c_{cell} that is necessary to solve the Nernst equation (3). Because the ion concentrations are not uniformly distributed inside the cell, we will make an approximation to determine c_{cell} from the mean value of c_{in} and c_{out}:

$$c_{cell_i}(t) = \frac{c_{in_i}(t) + c_{out_i}(t)}{2} \qquad [mol/l] \tag{18}$$

3.2 Concentration of protons

Unfortunately, (1) does not reflect exactly the phenomena happening in the cells. Indeed, the VRB electrolytes contain not only vanadium ions at different oxidation states, but also protons H^+ and sulphate ions SO_4^{2-} that are only partially represented in the chemical equations; these ions are called spectator ions and do not take an active part in the reaction. But these spectator ions are important to respect the law of conservation of mass and the charge balance in both electrolytes (Blanc, 2009). The complete ionic equation, illustrated in Fig. 5, is useful to understand how the protons concentration c_{H^+} changes and why the protons cross the membrane to balance the charge.

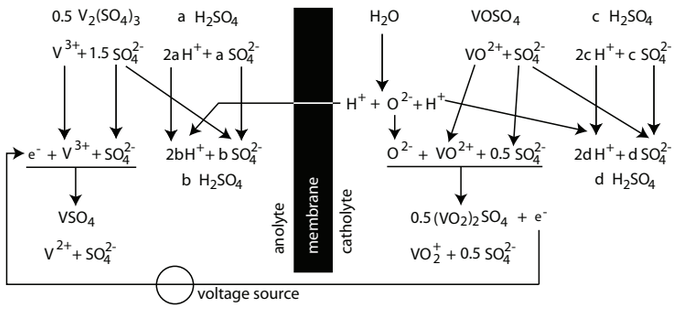

Fig. 5. Illustration of the full ionic equations of the VRB during the charge.

Hence, the protons concentration in the catholyte depends on the electrolyte composition and varies with the state of charge:

$$c_{H^+} = c_{H^+,discharged} + c_{VO^{2+}} \ [M] \tag{19}$$

where $c_{H^+,discharged}$ is the protons concentration when the electrolyte is completely discharged.

3.3 Internal losses

When a net current is flowing through the stack, the equilibrium conditions are not met anymore and the stack voltage U_{stack} is now given by the difference between the equilibrium potential U_{eq} and the internal losses U_{loss}. These losses are often called overpotentials and represent the energy needed to force the redox reaction to proceed at the required rate; a list of the variables affecting this rate is given in Fig. 6.

$$U_{loss}(t) = \eta_{act}(t) - \eta_{conc}(t) - \eta_{ohm}(t) - \eta_{ion}(t) \ [V] \tag{20}$$

The activation η_{act} and the concentration η_{conc} overpotentials are electrode phenomena and are respectively associated with the energy required to initiate a charge transfer and caused by concentration differences between the bulk solution and the electrode surface; in addition, the ohmic η_{ohm} and ionic η_{ionic} losses also alter the stack voltage. The ohmic losses η_{ohm} occur in the electrodes, the bipolar plates and the collector plates and the ionic losses η_{ionic} occur in the electrolytes and the membranes. But these overpotentials are seldom found in the literature and often applicable only to peculiar conditions. Therefore, an equivalent resistance is introduced instead:

$$U_{loss}(t) = R_{eq,charge/discharge} i(t) \ [V] \tag{21}$$

where $R_{eq,charge}$ is the equivalent charge resistance and $R_{eq,discharge}$ corresponds to the discharge resistance; these values are found experimentally (Skyllas-Kazacos & Menictas, 1997) and depends on the electrolyte, electrode materials and stack construction.

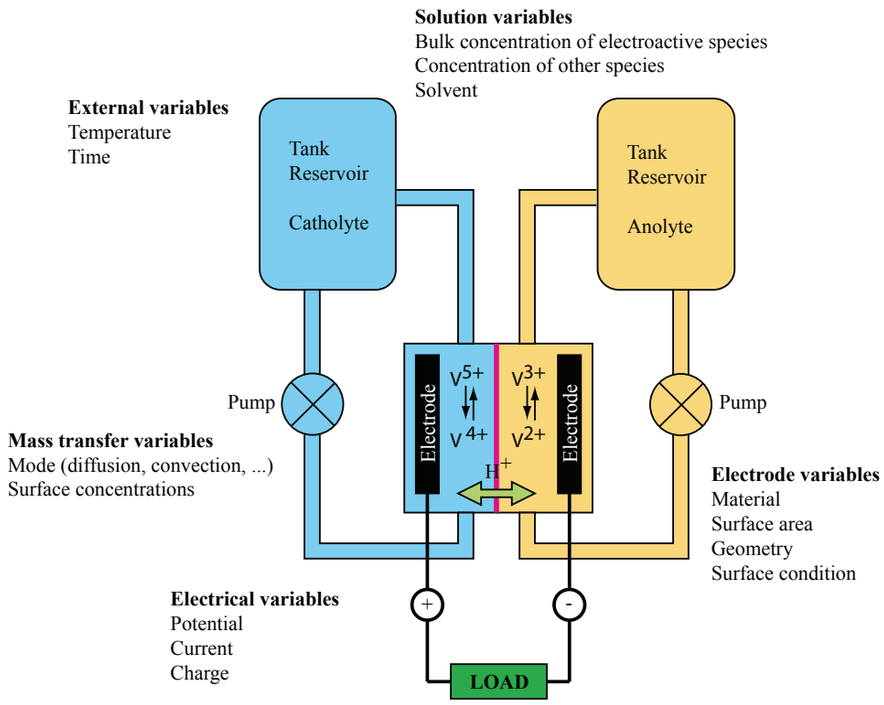

Fig. 6. Schematic representation of VRB with a list of variables affecting the rate of the redox reaction (Bard & Faulkner, 2001). Note that only one cell is represented on this figure.

3.4 State of charge

The state of charge SoC indicates how much energy is stored in the battery; it varies from 0 (discharged state) to 1 (charged) and is defined by the following relation:

$$SoC = \left(\frac{c_{V^{2+}}}{c_{V^{2+}} + c_{V^{3+}}} \right) = \left(\frac{c_{VO_2^+}}{c_{VO^{2+}} + c_{VO_2^+}} \right) \ [-] \tag{22}$$

3.5 Electrochemical model

From the principles explained in the previous section, it is now possible to introduced the electrochemical model that describes the behaviour of the stack, mainly how the stack voltage U_{stack} depends on the operating conditions: the current I, the vanadium concentrations in the electroactive cells c_{cell}, the protons concentration c_{H^+}, the electrolyte flowrate Q and the temperature T; furthermore, it also describes how the electrolyte compositions change as the battery is operating. The schematic representation of this model is shown in Fig. 7.

3.6 Efficiencies

Efficiencies are parameters used to assess the performance of storage system. Basically, the definition of efficiency is simple, the energy efficiency η_{energy} is the ratio of the energy furnished by the battery during the discharge to the energy supplied during the charge:

$$\eta_{energy} = \frac{\int P_{VRB,discharge}(t)dt}{\int \left| P_{VRB,charge} \right| (t)dt} \qquad [-] \tag{23}$$

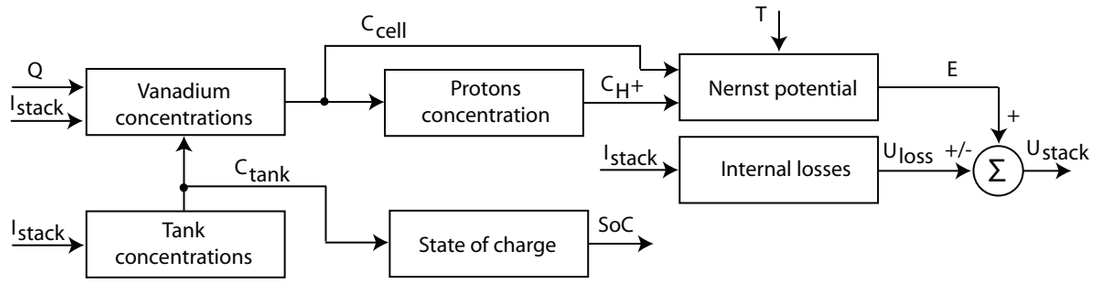

Fig. 7. Schematic representation of the electrochemical model

Name	Value	Name	Value
number of cells N_{cells}	19	electrolyte vanadium concentration	2 M
R_{charge}	0.037 Ω	tank size V_{tk}	83 l
$R_{discharge}$	0.039 Ω	initial concentration of vanadium species	1 M
electrolyte flowrate Q	2 l/s		

Table 3. The characteristics of the VRB stack.

But difficulties quickly arise when different technologies or products are compared because the operating mode has a significant impact on the performance: a quick charge produces more losses than a gentle one. The coulombic efficiency $\eta_{coulombic}$ is a measure of the ratio of the charge withdrawn from the system $Q_{discharge}$ during the discharge to the charge Q_{charge} supplied during the charge:

$$\eta_{coulombic} = \frac{Q_{discharge}}{Q_{charge}} = \frac{\int i_{discharge}(t)dt}{\int \left| i_{charge}(t) \right| dt} \qquad [-] \tag{24}$$

The voltage efficiency $\eta_{voltage}$ is defined for a charge and discharge cycle at constant current. It is a measure of the ohmic and polarisation losses during the cycling. The voltage efficiency is the ratio of the integral of the stack voltage $U_{stack,discharge}$ during the discharge to that of the voltage $U_{stack,charge}$ during the charge:

$$\eta_{voltage} = \frac{\int U_{stack,discharge}(t)dt}{\int U_{stack,charge}(t)dt} \neq \frac{\eta_{energy}}{\eta_{coulombic}} \qquad [-] \tag{25}$$

Note that when the mechanical losses P_{mech} are taken into account, $\eta_{voltage}$ is not equal to the ratio of η_{energy} to $\eta_{coulombic}$.

3.7 Charge and discharge cycles at constant current

The electrochemical model of the vanadium redox battery is compared in this section to experimental data. To determine the performance, a VRB composed of a 19 elements stack and two tanks filled with 83 l of electrolytes will be used. The total vanadium concentration in each electrolyte is 2 M. The characteristics of the stack are summarized in Tab. 3 and correspond to an experimental stack built by M. Skyllas-Kazacos and co-workers (Skyllas-Kazacos & Menictas, 1997). The electrochemical model is used to assess the stack efficiencies during a series of charge and discharge cycles at constant currents.

Current [A]	η_{energy} [%]	$\eta_{voltage}$ [%]	$\eta_{coulombic}$ [%]	Current [A]	η_{energy} [%]	$\eta_{voltage}$ [%]	$\eta_{coulombic}$ [%]
SIMULATION RESULTS				EXPERIMENTAL DATA			
10	97.0	97.0	100				
20	94.1	94.1	100				
40	88.6	88.6	100	60	78.3	82.8	94.6
60	83.3	83.3	100	100 (cycle 1)	68.0	72.3	94.0
80	78.4	78.4	100	100 (cycle 2)	70.8	73.0	96.1
100	73.7	73.7	100	100 (cycle 3)	73.1	74.0	98.7

Table 4. Efficiencies at various currents. The cycle starts at 2.5% SoC, the battery is charged until a 97.5% SoC and then discharged until a 2.5% SoC. Experimental data are from (Skyllas-Kazacos & Menictas, 1997).

At the beginning of the cycle, the battery state of charge SoC is 2.5% (discharged); the battery is charged at constant current until a SoC of 97.5% and then discharged until it reached its initial SoC. The resulting stack voltages U_{stack} and power P_{stack} are illustrated in Fig. 8 and the efficiencies are summarized in Tab. 4 along with experimental data. We observe quickly that the efficiencies decrease as the current increases.

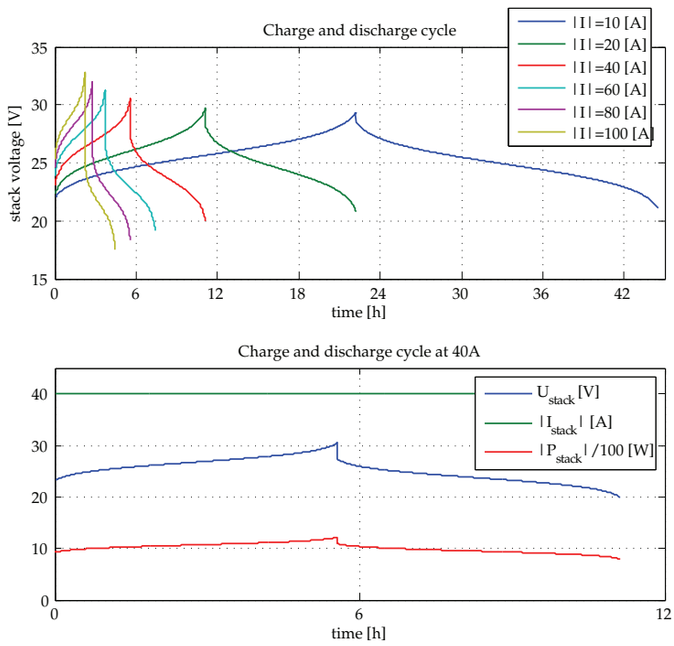

Fig. 8. Stack voltages during charge/discharge cycles at diverse currents. Below: stack voltage, current and power at 40A.

The voltage efficiencies $\eta_{voltage}$ are accurately determined by the model; the difference with the experimental data always stays below 2%. The losses in coulombic efficiency $\eta_{coulombic}$ can be caused by side reactions or cross mixing of electrolyte through the membrane which are not taken into account in the model; note that $\eta_{coulombic}$ has improved as the battery becomes conditioned. When $\eta_{coulombic}$ is close to 100%, as it is the case for the last cycle,

Solution of vanadium	Density [g/cm^3]	Viscosity [cP]	Vanadium / sulphuric acid concentration [M]
V^{2+}	1.2-1.3	1.7-2.4	1-2 / 2
V^{3+}	1.2-1.5	1.7-9.6	0.5-3 / 2
V^{4+}		(3.6-33.7)	0.25-3 / 3
V^{4+}	1.2-1.5		1-2 / 1-9
V^{5+}	1.2-1.5		1-2 / 1-9
V^{5+}		3.2-22.3	0.5-3 / 4-7

Table 5. Density and viscosity of vanadium species solutions (Mousa, 2003; Wen et al., 2006; Oriji et al., 2004; Kausar, 2002). The numbers in brackets are estimations made from the kinematic viscosity.

the experimental and simulated energy efficiencies η_{energy} are almost the same, the difference being less than 1%. In the worst case, cycle 1, the difference is around 8.3%.

4. Electrolyte properties

The electrolyte properties are important parameters in the mechanical model; the density indicates its inertia, or resistance to an accelerating force, and the viscosity describes its *fluidity*, it may be thought of as internal friction between the molecules. They are both related to the attraction forces between the particles; thus they depend on the electrolyte composition.
The VRB electrolytes are composed of vanadium ions dissolved in sulphuric acid; we have seen previously that their composition changes as the battery is operating (see Fig. 3). Therefore, the electrolyte properties must change accordingly to the composition; but for simplicity reasons, these properties are maintained constant in this work. Tab. 5 gives the density and the viscosity for some vanadium solutions.

5. Fluid mechanics applied to the vanadium redox flow batteries

We introduce in this section the mechanical model that determines the power P_{pump} required to flow the electrolytes from the tanks through the stack and back in the tanks (see Fig. 1). This model is composed of an analytical part that models the pipes, bends, valves and tanks and a numerical part that describes the more complex stack hydraulic circuit.

5.1 Hydraulic circuit model (without the stack)

The analytical hydraulic model describes the pressure drop Δp_{pipe} in the pipes, the valve and the tank; it is based on the extended Bernoulli's equation that relates Δp_{pipe} to the fluid velocity V_s, the height z, the head loss h_f due to the friction and the minor losses h_m:

$$\Delta p_{pipe} = -\gamma \left(\frac{\Delta V_s^2}{2g} + \Delta z + h_f + h_m \right) \qquad [Pa] \tag{26}$$

where γ is the specific weight and g the gravitational acceleration.
The head losses are obtained by dividing the hydraulic circuit into smaller sections where $h_{f,i}$ or $h_{m,i}$ are easily determined with the Darcy-Weisbach equation (Munson et al., 1998):

$$h_{f,i} = f_i \frac{L_i}{D_i} \frac{V_{s,i}^2}{2g}, \quad h_{m,i} = k_{L,i} \frac{V_{s,i}^2}{2g} \qquad [m] \tag{27}$$

geometry	Loss coefficient $k_{L,i}$
from a reservoir into a pipe	0.04 - 0.9
from a pipe into a reservoir	1
bends and elbows	0.2 - 1.5
valves	0.15 - 10

Table 6. Loss coefficients (Munson et al., 1998; Candel, 2001).

where f_i is the friction factor, $k_{L,i}$ the loss coefficient given in Tab. 6, L_i and D_i are the length and diameter of the conduit.
When the flow is laminar, the friction factor f_i is derived from the Poiseuille law (28) and for a turbulent flow, it is obtained from the Colebrook equation (29) (Candel, 2001):

$$f_i = \frac{64}{Re_i} \qquad [-] \tag{28}$$

$$\frac{1}{\sqrt{f_i}} = -2\log\left(\frac{\epsilon_i}{3.7D_i} + \frac{2.51}{Re_i\sqrt{f_i}}\right) \qquad [-] \tag{29}$$

where ϵ_i is the equivalent roughness of the pipe and Re_i is the Reynolds number:

$$Re = \frac{\rho V_s D}{\mu} = \frac{V_s D}{\nu} \qquad [-] \tag{30}$$

where ρ is the density, μ the dynamic viscosity and ν the kinematic viscosity.

5.2 Stack hydraulic model

The stack geometry is too complex to be analytically described (Fig. 9), therefore the stack hydraulic model can only be numerically obtained with a finite element method (FEM).

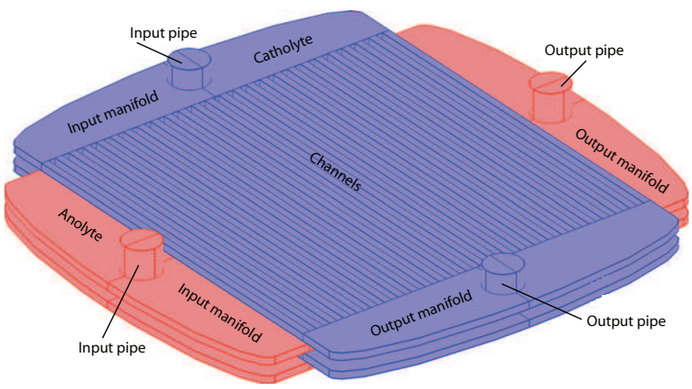

Fig. 9. Hydraulic circuit of a 2 cells stack. Note that the frame is not represented and that the colored segments represented the electrolytes (liquid).

It was assumed that the flow stays laminar in the stack; although the flow might be turbulent in the manifold at high velocity. In this example, the flow stays laminar in the distribution channels where the major part of the pressure drop Δp_{stack} occurs; therefore, the pressure drop in the stack Δp_{stack} is proportional to the flowrate:

$$\Delta p_{stack} = Q\widetilde{R} \qquad [Pa] \tag{31}$$

where $\widetilde{R}$ is the hydraulic resistance obtained from FEM simulations.

5.3 Mechanical model

Finally, the sum of the pressure drop in the pipes Δp_{pipe} and the pressure drop in the stack Δp_{stack} determines the hydraulic circuit pressure drop Δp_{system}:

$$\Delta p_{system} = \Delta p_{pipe} + \Delta p_{stack} \qquad [Pa] \tag{32}$$

The pump power P_{pump}, a determinant variable that influences the battery performance is related the head rise h_p supplied by the pump, to the fluid density γ and to the flowrate Q; we can also relate it to the pressure drop Δp (Wilkes, 2005):

$$P_{pump} = \gamma h_p Q = \Delta p \; Q \qquad [W] \tag{33}$$

The efficiency of the pump η_{pump} is affected by the hydraulic losses in the pump, the mechanical losses in the bearings and seals and the volumetric losses due to leakages inside the pump. Although η_{pump} is not constant in reality, it is assume in this work. Therefore, the effective power required by the pump P_{mech} is given by:

$$P_{mech} = \frac{P_{pump}}{\eta_{pump}} \qquad [W] \tag{34}$$

Thus, the relations introduced in this section can be combined to form the mechanical model of the VRB as illustrated in Fig. 10. Remember that the VRB needs two pumps to operate.

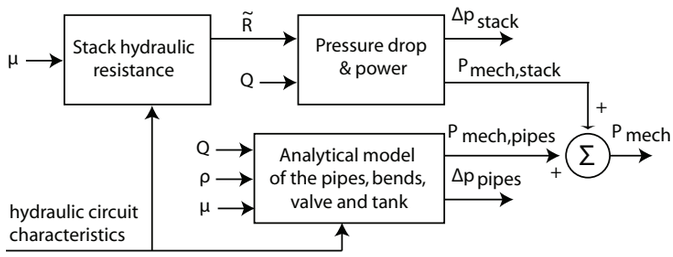

Fig. 10. Flowchart of the VRB mechanical model.

6. Multiphysics model and energetic considerations

The combination of the electrochemical model and the mechanical model leads to the multiphysics VRB system model. The functions that determine the vanadium concentrations in the tank c_{tank} and the state of charge SoC have been separated from the electrochemical model in order to be incorporated into a new model named *reservoir and electrolyte model*. A system control has also been added to supervise the battery operation; this system controls the flowrate Q and the stack current I_{stack}. This multiphysics system model, illustrated in Fig. 11, is a powerful means to understand the behaviour of the VRB, identify and quantify the sources of losses in this storage system; thus this multiphysics model is a good means to enhance the overall VRB efficiency.

6.1 Power flow

In order to optimize the performance of the VRB, it is important to understand the power flows within the VRB storage system. The power converters represented in Fig. 12 are necessary to adapt the stack voltage U_{stack} to the power source U_{grid} or to the load voltage U_{load} and to supply the mechanical power required to operate the pumps. Since power

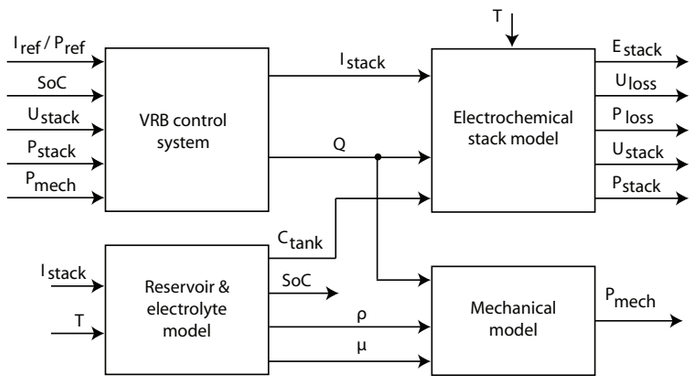

Fig. 11. Structured diagram of the multiphysics VRB system model.

converters are very efficient, with efficiencies around 98 to 99% (Wensong & Lai, 2008; Burger & Kranzer, 2009), they are considered, for simplicity, lossless in this work. Therefore, they are two sources of losses: the internal losses that are already included in the stack voltage U_{stack} (2), and the mechanical losses P_{mech}. Hence, P_{mech} is provided from the external power source during the charge and from the stack during the discharge. By convention, the battery power P_{VRB} and the stack power P_{stack} are positive during the discharge and negative during the charge; P_{mech} is always positive. Thus, P_{VRB} is given by:

$$P_{VRB} = P_{stack} - P_{mech} \qquad [W] \tag{35}$$

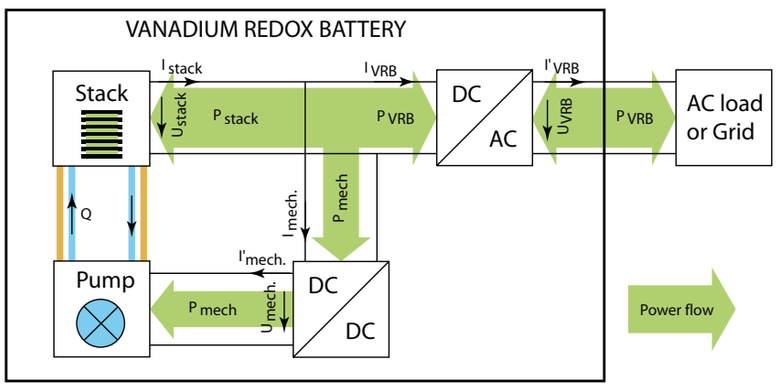

Fig. 12. Power flow in the VRB storage system. In this example, the power converters only adapt the currents and voltages, and are lossless.

In the rest of this section, we will discuss the battery performance under different operating strategy with a strong focus on the battery power P_{VRB}, the stack power P_{stack} ant the mechanical power P_{mech}. Intuitively, we feel that there should be an optimal control strategy that maximizes the battery performance. In these circumstances, the power delivered to the battery at any operating point is minimized during the charge and the power supplied by the battery is maximized during the discharge.

7. Operation at maximal and minimal flowrates

First, we will discuss the battery operation at maximal and minimal flowrates. We must keep in mind that an efficient control strategy must maximize the power exchanged with the battery

Name	Value
number of cells N_{cells}	19
R_{charge}	0.037 Ω
$R_{discharge}$	0.039 Ω
flow resistance $\widetilde{R}$	14186843 Pa/m^3
electrolyte vanadium concentration	2 M
tank size V_{tank}	83 l
initial concentration of vanadium species	1 M

Table 7. the parameters of the simulation.

while minimizing the losses; there is no point to have a battery that consumes more power than necessary. To illustrate this discussion, we will use a 2.5 kW, 6 kWh VRB in the rest of this chapter; its characteristics are summarized in Tab. 7.

7.1 Maximal flowrate

The simplest control strategy operates the battery at a constant flowrate set to provide enough electroactive species to sustain the chemical reaction under any operating conditions. Therefore, this flowrate Q_{max} is determined by the worst operating conditions: low state of charge SoC during the discharge and high SoC during the charge at high current in both cases. For the battery described in Tab. 7, Q_{max} is around 1.97 l/s: in that case, the mechanical power P_{mech} is 1720 W. In order to assess the performance, an instantaneous battery efficiency $\eta_{battery}$ is defined as follow:

$$\eta_{battery} = \frac{|P_{stack}|}{|P_{stack}| + P_{mech}} \qquad [-] \tag{36}$$

Clearly, the battery performance is poor as it can be observed in Fig. 14 where $\eta_{battery}$ is illustrated as a function of the stack current I_{stack} and the state of charge SoC. Indeed, the battery often consumes more power than necessary; therefore, constantly operating the battery at Q_{max} is not a wise strategy. Nevertheless, it is possible to improve this efficiency by limiting the operating range of the battery (smaller current and/or narrower state of charge); thus the flowrate Q_{max} and the mechanical power P_{mech} are reduced. But this also reduces the power rating and/or the energetic capacity while it increases the cost.

7.2 Minimal flowrate

The low efficiency at constant flowrate Q_{max} is due to the large mechanical losses P_{mech}; therefore, a second control strategy is proposed to minimize P_{mech}. In that case, the battery is operating at a minimal flowrate Q_{min} that is constantly adapted to the actual operating conditions (SoC and I_{stack}) in order to supply just enough electroactive materials to fuel the electrochemical reactions. Since the vanadium concentrations c_V change proportionally to I_{stack}, there are critical operating points where c_V is close to its boundary. In some cases, the variations of vanadium concentrations tend toward the limit values (Fig. 13). In these critical regions, the electrolyte flowrate Q must be larger to palliate the scarcity of electroactive vanadium ions.

Hence, the minimal flowrate Q_{min} depends on the required amount of electroactive species, and in consequence on I_{stack}, and on the input vanadium concentrations c_{in} that are either

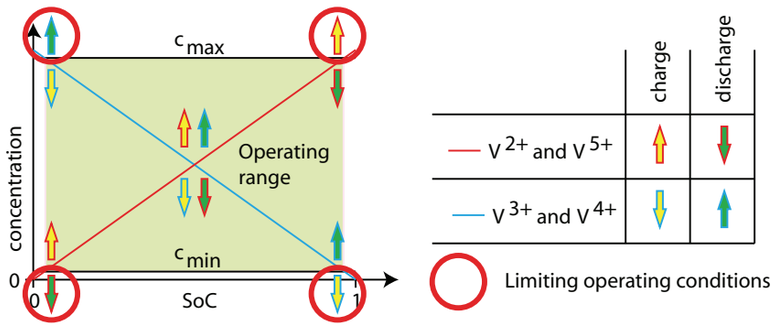

Fig. 13. Operating range and limiting operating conditions. The arrows represent the direction of the vanadium concentrations change as a function of the battery operating mode. The critical operating regions are highlighted in red; they represent the regions where the vanadium concentration $c_{vanadium}$ tends to its limiting concentrations (c_{max} or c_{min}).

being depleted ($\downarrow$) or augmented ($\uparrow$). Q_{min} can be derived from (17):

$$Q_{min,\downarrow}(t) = \frac{bN_{cell}i(t)}{F(c_{out,min} - c_{in,\downarrow}(t))} \qquad [l/s] \tag{37}$$

$$Q_{min,\uparrow}(t) = \frac{bN_{cell}i(t)}{F(c_{out,max} - c_{in,\uparrow}(t))} \qquad [l/s] \tag{38}$$

where $c_{out,min}$ and $c_{out,max}$ are constant minimal and maximal output concentrations. The limiting species depends on the operating mode (charge or discharge); thus Q_{min} is given by the maximal value of (37) and (38):

$$Q_{min}(t) = \max\left(Q_{min,\downarrow}(t), Q_{min,\uparrow}(t)\right) \qquad [l/s] \tag{39}$$

Q_{min} is illustrated in Fig. 14 for a wide spectrum of operating points; clearly, Q_{min} is larger in the critical regions that were highlighted in Fig. 13. Moreover, Q_{min} is, in comparison, very small in the other operating regions; therefore, there must be a large benefit to operate the battery at Q_{min}.

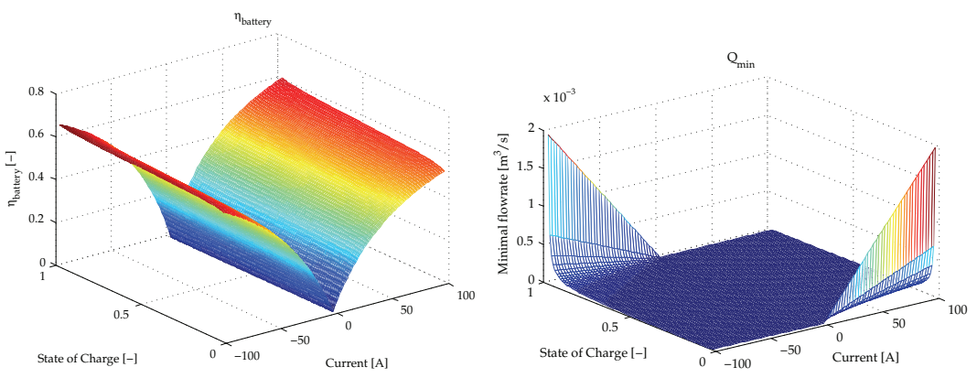

(a) (b)

Fig. 14. (a) The battery efficiency $\eta_{battery}$ at constant flowrate Q_{max} as a function of the state of charge SoC and current I. (b) Minimal flowrate Q_{min} as a function of the stack current I_{stack} and the state of charge SoC.

But a change in the flowrate Q also modifies the vanadium concentrations c_{cells} within the cells according to (18), and in consequence the stack voltage U_{stack} and power P_{stack} according to (2) and (3). This phenomenon is illustrated in Fig. 15 where the equilibrium voltage E at Q_{max} and Q_{min} is shown: an increase of the flowrate has always a beneficial effect on E. Furthermore, the equivalent state of charge SoC_{eq} which represents the SoC of the electrolyte within the cells is also illustrated as a function of Q. Clearly, SoC_{eq} tends toward the battery SoC at high Q. Therefore, the change in c_{cells} is maximal at Q_{min}; and consequently a large variation of U_{stack} and P_{stack} is expected between the operations at Q_{min} and Q_{max} as it can be observed in Fig. 16. From the strict point of view of P_{stack}, it is more interesting to operate the battery at Q_{max}; indeed, more power is delivered during the discharge and less is consumed during the charge. But it will be shown in the next sections that the mechanical power greatly deteriorates the performance and that the energy efficiency at Q_{max} is unacceptable.

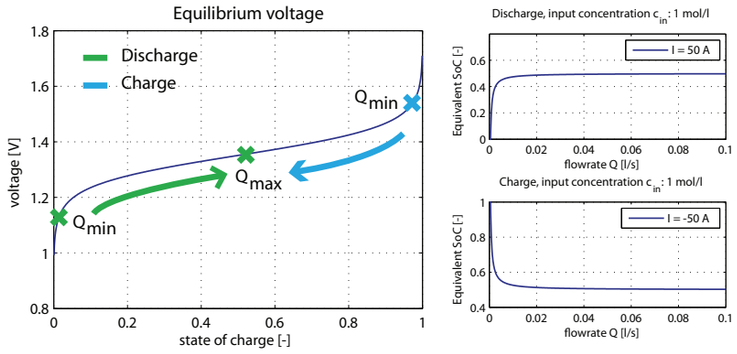

Fig. 15. Effect of the flowrate Q on the equilibrium voltage E. On the right, the variation of the equivalent state of charge SoC as a function of Q during the discharge and the charge. In this example, the battery SoC is 0.5, i.e. the input concentrations are 1 M for each vanadium species.

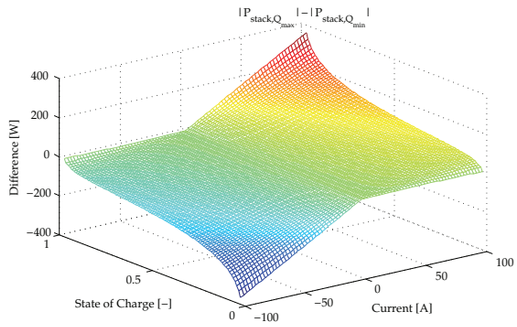

Fig. 16. The difference between the stack power $\left|P_{stack,Qmax}\right|$ at Q_{max} and the stack power $\left|P_{stack,Qmin}\right|$ at Q_{min}.

8. Optimal operating point at constant current

In the previous sections, the advantages and disadvantages of operating the battery at either Q_{max} and Q_{min} were discussed. At Q_{max}, the stack power P_{stack} has the highest possible value but the mechanical power P_{mech} is also very large and consequently deteriorates the performance. At Q_{min}, P_{mech} is reduced to the minimum, but P_{stack} is negatively affected.

Therefore, it should exist an optimal flowrate Q_{opt} somewhere between Q_{min} and Q_{max} that increases P_{stack} while maintaining P_{mech} at a small value.

8.1 Optimal flowrate during the discharge

In this section, the battery is controlled by the reference current $I_{stack,ref}$; therefore there is only one control variable: the flowrate Q. Indeed, the stack power P_{stack} depends on I_{stack}, Q and the state of charge SoC whereas the mechanical power depends on Q and the electrolyte properties: the density ρ and the viscosity μ that are maintained constant in this work. During the discharge, the optimal operating point is found when the flowrate Q_{opt} maximizes the power delivered by the stack P_{stack} while minimizing the mechanical power P_{mech}. When these conditions are met together, the power delivered by the battery P_{VRB} is optimized:

$$\max(\underbrace{P_{VRB}}_{f(U_{stack},I_{VRB})}) = \max(\underbrace{P_{stack}}_{f(I_{stack},Q,SoC)} - \underbrace{P_{mech}}_{f(Q,\mu,\rho)}) \tag{40}$$

In Fig. 17, P_{VRB} is represented during the discharge as a function of Q at different states of charge for a current of 100 A. Clearly, an optimal flowrate Q_{opt} exists between Q_{min} and Q_{max} that maximizes P_{VRB}. The shape of the curves can be generalized to other discharge currents $I_{stack} > 0$; although in some cases where I_{stack} is low, P_{VRB} might become negative at inappropriately high flowrate Q.

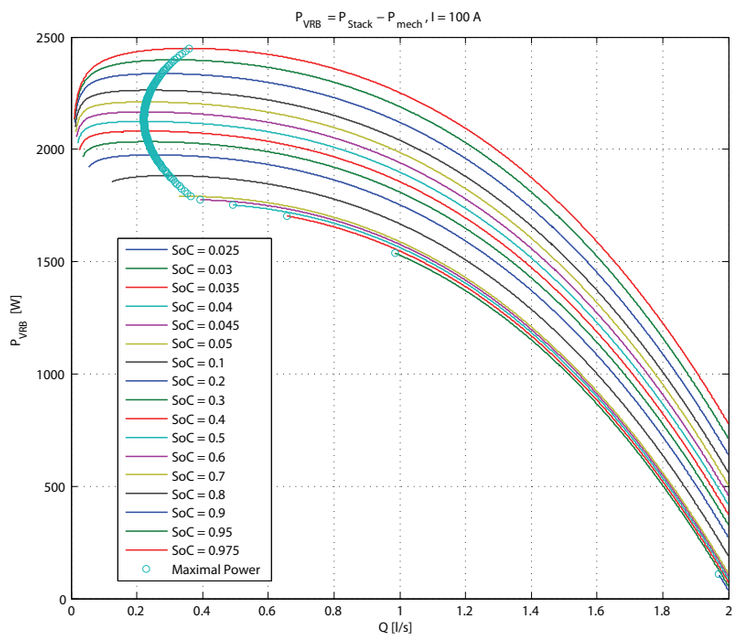

Fig. 17. Optimal flowrate Q_{opt} as a function of the flowrate Q and the state of charge SoC. Note that when SoC is low, Q_{opt} is equal to the minimal flowrate Q, and the discharge current is equal to 100 A.

8.2 Optimal flowrate during the charge

At constant current $I_{stack,ref}$, the quantity of electrons e^- stored in the electrolyte does not depend on the stack power P_{stack} but solely on the stack current I_{stack}; therefore, there is no reason to have a high P_{stack}. Hence, the optimal flowrate Q_{opt} during the charge is found

when the sum of P_{stack} and P_{mech} is simultaneously minimal. This condition is expressed by the following relation[3]:

$$\min(\underbrace{|P_{VRB}|}_{f(U_{stack},I_{VRB})}) = \min(\underbrace{|P_{stack}|}_{f(I_{stack},Q,SoC)} + \underbrace{P_{mech}}_{f(Q,\mu,\rho)}) \tag{41}$$

The optimal flowrate Q_{opt} is illustrated in Fig. 18 where P_{VRB} is shown as a function of Q and SoC. At very high SoC, Q_{opt} is equal to Q_{min} because the electrolyte carries a very small amount of electroactive vanadium ions. Again, the shape of the curves can be generalized to other charge currents $I_{stack} < 0$.

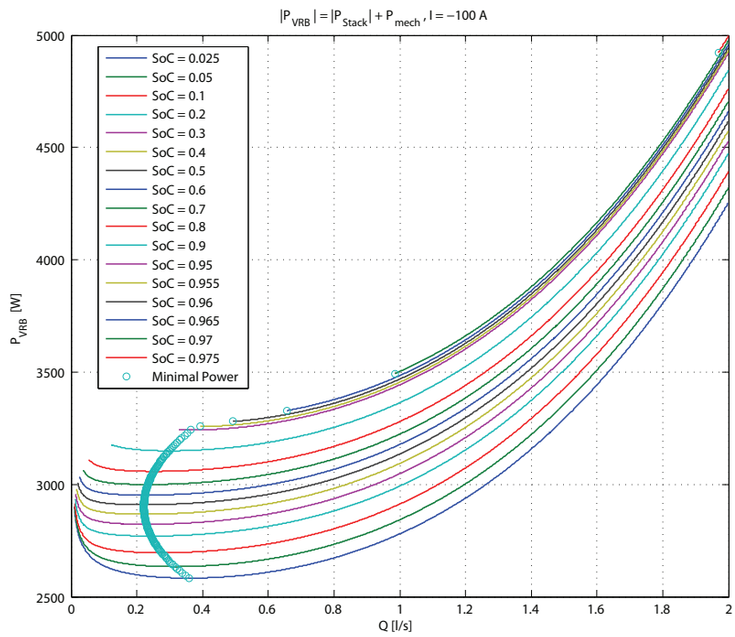

Fig. 18. Optimal flowrate Q_{opt} as a function of the flowrate Q and the state of charge SoC. Note that when SoC is high, Q_{opt} is equal to the minimal flowrate Q, and that the charge current I_{stack} is equal to -100 A.

8.3 Charge and discharge cycles

It is always difficult to assess the performance of a battery because it often depends on the operating conditions. In this section, a series of charge and discharge at constant current is performed at minimal flowrate Q_{min}, at maximal flowrate Q_{max} and at optimal flowrate Q_{opt} in order to assess the performance of this new control strategy.

The voltage $\eta_{voltage}$ and energy η_{energy} efficiencies are summarized in Tab. 8 and 9; the coulombic efficiency $\eta_{coulombic}$ is in all cases equal to 100% because the model does not take into account any side reactions such as oxygen or hydrogen evolution nor any cross mixing of the electrolyte.

Both $\eta_{voltage}$ and η_{energy} decrease when the current increase; this is mainly due to the internal losses U_{losses} that are proportional to the current I_{stack}, although the flowrates Q_{min} and Q_{opt} increases to supply enough electroactive species. The highest voltage efficiencies occur

[3] A close look at this relation reveals that it is the same as (40), but (41) is more intuitive for the charge.

Current [A]	$\eta_{voltage,Qmax}$ [%]	$\eta_{voltage,Qmin}$ [%]	$\eta_{voltage,Qopt}$ [%]
10	97.02	87.74	96.69
20	94.13	85.11	93.70
40	88.58	80.09	88.03
60	83.33	75.31	82.69
80	78.37	70.78	77.68
100	73.65	66.46	72.94

Table 8. Stack voltage efficiency $\eta_{voltage}$ at constant maximal flowrate Q_{max}, at minimal flowrate Q_{min} and at optimal flowrate Q_{opt}.

Current [A]	Time [h]	$\eta_{energy,Qmax}$ [%]	$\eta_{energy,Qmin}$ [%]	$\eta_{energy,Qopt}$ [%]
10	44.49	-73.42	87.73	96.54
20	22.24	-53.34	85.10	93.51
40	11.12	-25.65	80.04	87.77
60	7.41	-8.17	75.31	82.34
80	5.56	3.24	70.78	77.26
100	4.45	10.81	66.24	72.43

Table 9. Overall VRB energy efficiencies η_{energy} at constant maximal flowrate Q_{max}, at minimal flowrate Q_{min} and at optimal flowrate Q_{opt}.

at Q_{max} because of its positive effect on the stack voltage U_{stack} highlighted in section 7.2; consequently, the worst voltage efficiencies occur at Q_{min}. Moreover, the voltage efficiencies at Q_{opt} are very close to the maximal efficiencies obtained at Q_{max}. In fact, the stack voltages $U_{stack,Qmax}$ and $U_{stack,Qopt}$ are very close as it can be observed in Fig. 19.

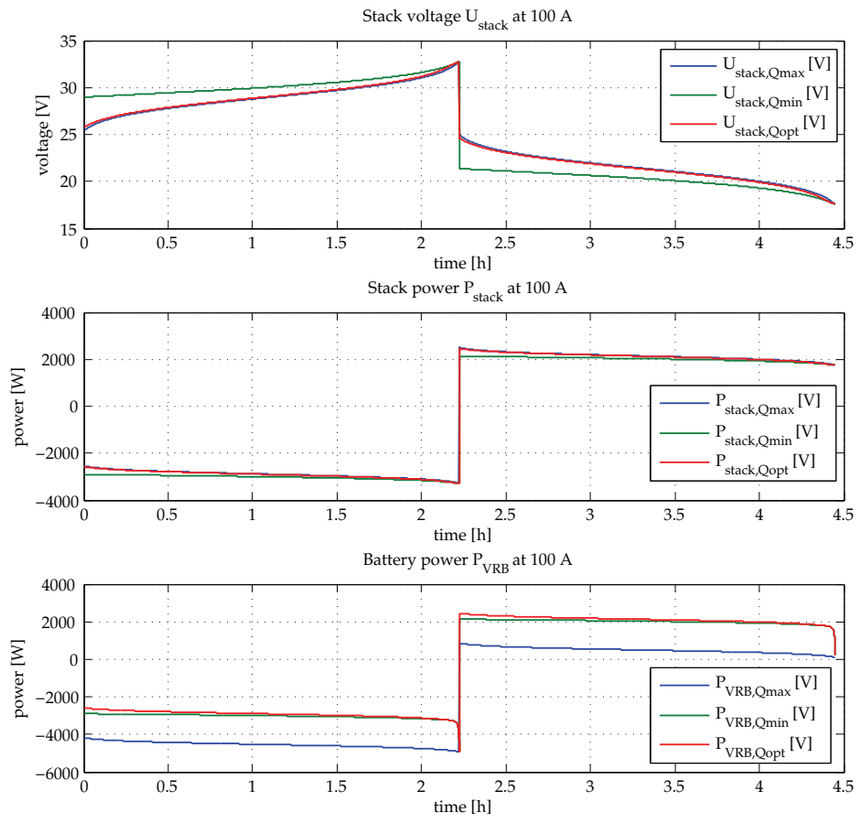

Fig. 19. Stack voltage U_{stack}, stack power P_{stack} and battery power P_{VRB} during a charge and discharge cycle at 100 A.

Obviously, operating the battery at Q_{max} is a problematic strategy as $\eta_{energy,Qmax}$ is very small or even negative: at small currents, the battery does not deliver any power to the load but consumes more power to operate the pumps than the stack is furnishing. When P_{mech} is minimized, the energy efficiencies already become interesting at Q_{min}, but they are increased by a further 10% when the battery is operating at Q_{opt}.
In order to compare the model with experimental data, the stack characteristics were defined to match the stack presented in section 3.7. The experimental results of M. Skyllas-Kazacos and al. are summarized in Tab. 4 (Skyllas-Kazacos & Menictas, 1997); note that they do not take into account the mechanical power required to operate the pumps and that the flowrate was constant (2 l/s which correspond to Q_{max}). The losses in coulombic efficiency $\eta_{coulombic}$ can be caused by side reactions or cross mixing of electrolyte through the membrane which are not taken into account in the model; but $\eta_{coulombic}$ improves as the battery becomes conditioned. In that case, the energy efficiency $\eta_{energy,Qopt}$ at optimal flowrate is very close to the maximal electrochemical energy efficiency. Finally, a very good concordance is observed between the voltage efficiencies at Q_{max} and the experimental results.

9. Optimal operating point at constant power

In practice, the battery must often deliver a certain amount of power to the load: the battery is controlled by a reference power P_{ref}. In that case, a second control variable is available in supplement of the flowrate Q: the stack current I_{stack}. The optimal operating point is the couple Q_{opt} and I_{opt} that maximizes the amount of charge that are stored within the electrolyte during the charge and minimizes the amount of charge that are consumed during the discharge. These conditions can be related to I_{stack}:

$$\underbrace{P_{VRB}}_{constant} = \underbrace{P_{stack}}_{f(I_{stack},Q,SoC)} - \underbrace{P_{mech}}_{f(Q,\mu,\rho)} \quad [W] \tag{42}$$

$$\begin{aligned} \text{during the charge: } & \max(|I_{stack}|) \quad [A] \\ \text{during the discharge: } & \min(I_{stack}) \quad [A] \end{aligned} \tag{43}$$

Again, an optimal operating point exists in between the maximal Q_{max} and minimal Q_{min} flowrates as it can be observed in Fig. 20 where operating points are represented for different battery power P_{VRB} during the discharge at a SoC equal to 0.5. At the optimal flowrate Q_{opt}, the battery delivers the same power P_{VRB} but consumes less active vanadium ions; therefore, the battery will operate longer and deliver more power. Q_{opt} increases with P_{VRB} until it reaches a plateau due to the transition between the laminar and the turbulent regime.

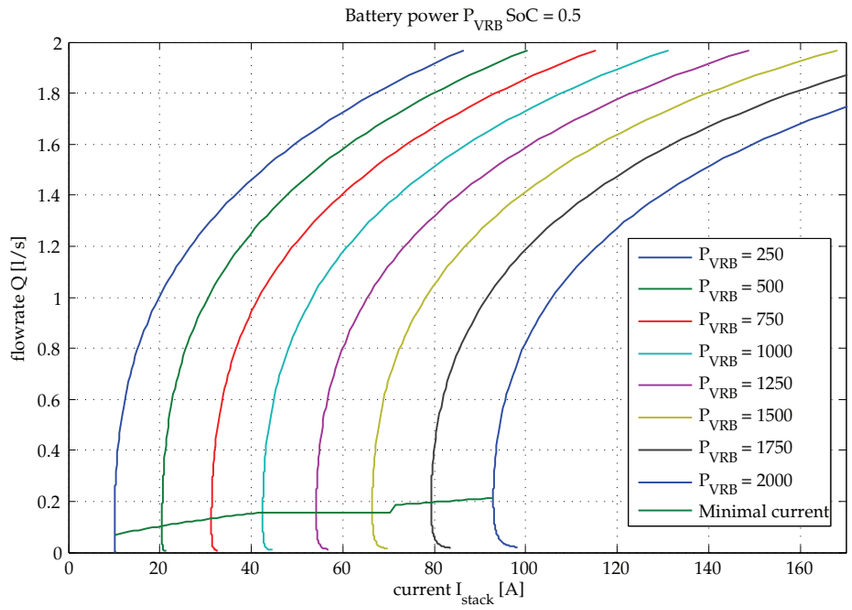

Fig. 20. Battery power P_{VRB} as a function of the discharge current I_{stack} and the electrolyte flowrate Q at a state of charge SoC equal to 0.5. The optimal operating points occurs when the current I_{stack} is minimal for a given battery power P_{VRB}.

In fact, I_{stack} increases above the optimal flowrate to compensate the higher mechanical loss: the stack must deliver more power. Below Q_{opt}, I_{stack} increases this time to compensate the lower stack voltage U_{stack} due to the lower concentrations of active species. The shape of the curves can be generalized for other states of charge SoC.
The optimal operating points during the charge are illustrated in Fig. 21 where the battery power P_{VRB} is shown as a function of the current I_{stack} and the flowrate Q at a state of charge

of 0.5. The optimal operating point maximizes the current $|I_{stack}|$ delivered to the stack in order to store the maximum amount of electroactive species at a given power $P_{VRB,ref}$; again, the optimal flowrate Q_{opt} increases with the battery power P_{VRB} until it reaches the plateau due to the flow regime transition.

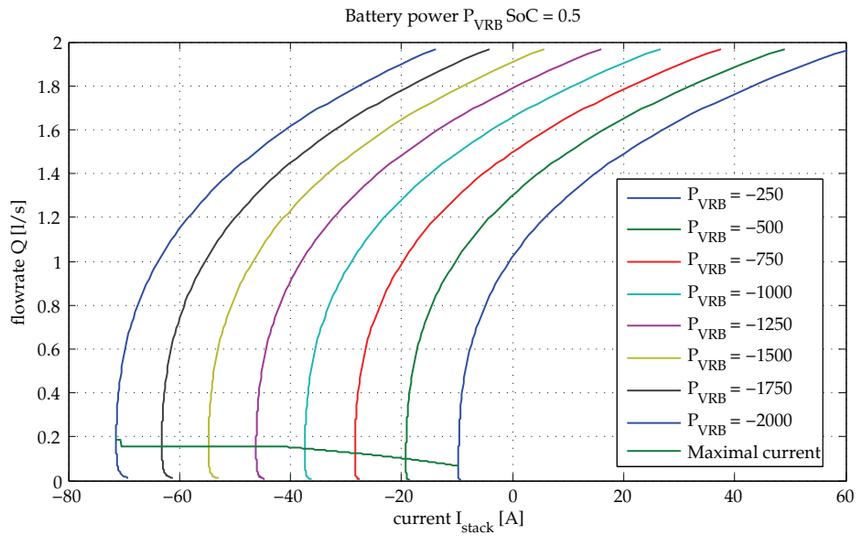

Fig. 21. Battery power P_{VRB} as a function of the charge current I_{stack} and the electrolyte flowrate Q at a state of charge SoC equal to 0.5. The optimal operating points occurs when the current $|I_{stack}|$ is maximal for a given battery power P_{VRB}.

Interestingly, we observe in Fig. 21 that the stack current I_{stack} changes its sign at high flowrate Q; in these unacceptable conditions, the stack is discharged while the battery is being charged. During the charge, the stack current $|I_{stack}|$ decreases above the optimal flowrate Q_{opt} to compensate the higher mechanical loss P_{mech}; in consequence, less power is available to charge the stack (see (42)). Below the optimal flowrate Q_{opt}, the stack current $|I_{stack}|$ also decreases because the stack voltage U_{stack} increases due the change in electroactive species concentrations within the cells c_{cell}; note that the mechanical power P_{mech} is also reduced below Q_{opt}. Furthermore, the shape of the curves in Fig 21 might be generalized to other states of charge SoC.

9.1 Charge and discharge cycles

A new series of charge and discharge cycles at constant power was performed to determine the energy efficiencies at minimal flowrate Q_{min} and at the optimal operating point: I_{opt} and Q_{opt}. This optimal point is constantly determined as a function of the actual conditions. The energy efficiencies are given in Tab. 10. The energy efficiency at optimal flowrate $\eta_{energy,Qopt}$ is increased by 10% at maximal power when compared to battery operations at minimal flowrate Q_{min}.

10. Epilogue

Today, the electricity industries are facing new challenges as the market is being liberalized and deregulated in many countries. Unquestionably, electricity storage will play, in the near future, a major role in the fast developing distributed generations network as it has

Power [W]	$\eta_{energy,Qmin}$ [%]	$\eta_{energy,Qopt}$ [%]
500	87.07	93.59
1000	81.04	87.78
1500	75.47	82.09
2000	69.91	76.39
2500	63.97	70.48

Table 10. Overall VRB energy efficiencies η_{energy} for a charge and discharge cycle at constant power at either optimal flowrate Q_{opt} and minimal flowrate Q_{min}.

many advantages to offer: management of the supply and demand of electricity, power quality, integration of renewable sources, improvement of the level of use of the transport and distribution network, etc. Over the years, many storage technologies have been investigated and developed, some have reached the demonstrator level and only a few have become commercially available. The pumped hydro facilities have been successfully storing electricity for more than a century; but today, appropriate locations are seldom found. Electrochemical storage is also an effective means to accumulate electrical energy; among the emerging technologies, the flow batteries are excellent candidates for large stationary storage applications where the vanadium redox flow battery (VRB) distinguishes itself thanks to its competitive cost and simplicity.

But a successful electricity storage technology must combine at least three characteristics to have a chance to be widely accepted by the electrical industry: low cost, high reliability and good efficiency. A lot of works have already been done to improve the electrochemistry of the VRB and to reduce its overall manufacturing cost. With the multiphysics model proposed in this chapter, we are able to address primarily the battery performance and indirectly its cost; indeed, a good efficiency enhances the profitability and consequently reduces the operating cost.

This ambitious model encompasses the domains of electricity, electrochemistry and fluid mechanics, it describes the principles and relations that govern the behaviour of the VRB under any set of operating conditions. Furthermore, this multiphysics model is a powerful means to identify and quantify the sources of losses within the VRB storage system; indeed, we are now able to understand how the VRB operates and to propose strategies of control and operation for a greater effectiveness of the overall storage system.

Another important feature of this multiphysics model is to facilitate the integration of the VRB into the electrical networks. Indeed, power converters, whose properties and characteristics are known and efficient, are required in practice to interface the VRB with the network; the overall performance might improve if their control strategy takes into account the VRB characteristics.

11. References

Bard, A. & Faulkner, L. (2001). *Electrochemical Methods, Fundamentals and Applications*, 2nd edn.

Bard, A., Parsons, R. & Jordan, J. (1985). *Standard Potentials in Aqueous solution*.

Bartolozzi, M. (1989). Development of redox flow batteries. a historical bibliography, *Journal of Power Sources* 27.

Blanc, C. (2009). *Modeling of a Vanadium Redox Flow Battery Electricity Storage System*, Ph. D. dissertation, EPFL.

Burger, B. & Kranzer, D. (2009). Extreme high efficiency pv-power converters, *EPE 2009 - Barcelona* .

Candel, S. (2001). *Mcanique des Fluides*.

Heintz, A. & Illenberger, C. (1998). Thermodynamics of vanadium redox flow batteries - electrochemical and calorimetric investigations, *Ber. Bunsenges. Phys. Chem.* 102.

Kausar, N. (2002). Studies of V(IV) and V(V) species in vanadium cell electrolyte, *PhD thesis, UNSW, Australia* .

Mousa, A. (2003). Chemical and electrochemical studies of V(III) and V(II) solutions in sulfuric acid solution for vanadium battery applications, *PhD thesis, UNSW, Australia* .

Munson, B., Young, D. & Okiishi, T. (1998). *Fundamentals of Fluid Mechanics*, third edn.

Oriji, G., Katayama, Y. & Miura, T. (2004). Investitgation on V(IV)/V(V) species in a vanadium redox flow battery, *Electrochimica Acta* 49.

Skyllas-Kazacos, M. & Menictas, C. (1997). The vanadium redox battery for emergency back-up applications, *Intelec 97* .

Sum, E., Rychcik, M. & Skyllas-Kazacos, M. (1985). Investigation of the V(V)/V(VI) system for use in the positive half-cell of a redox battery, *Journal of Power Sources* 16.

Sum, E. & Skyllas-Kazacos, M. (1985). A study of the V(II)/V(III) redox couple for redox flow cell applications, *Journal of Power Sources* 15.

Van herle, J. (2002). *Electrochemical Technology, Fuel Cells and Batteries, postgrade course*.

Wen, Y., Zhang, H., Qian, P., Zhao, P., Zhou, H. & Yi, B. (2006). Investigation on the electrode process of concentrated V(IV)/V(V) species in a vanadium redox flow battery, *Acta Physico-Chimica Sinica* 22.

Wensong, Y. & Lai, J.-S. (2008). Ultra high efficiency bidirectional dc-dc converter with multi-frequency pulse width modulation, *IEEE Applied Power Electronics Conference and Exposition, APEC 2008* .

Wilkes, J. (2005). *Fluid mechanics for chemical engineers*.

Paths to Sustainable Energy
Edited by Dr Artie Ng

ISBN 978-953-307-401-6
Hard cover, 664 pages
Publisher InTech
Published online 30, November, 2010
Published in print edition November, 2010

The world's reliance on existing sources of energy and their associated detrimental impacts on the environment- whether related to poor air or water quality or scarcity, impacts on sensitive ecosystems and forests and land use - have been well documented and articulated over the last three decades. What is needed by the world is a set of credible energy solutions that would lead us to a balance between economic growth and a sustainable environment. This book provides an open platform to establish and share knowledge developed by scholars, scientists and engineers from all over the world about various viable paths to a future of sustainable energy. It has collected a number of intellectually stimulating articles that address issues ranging from public policy formulation to technological innovations for enhancing the development of sustainable energy systems. It will appeal to stakeholders seeking guidance to pursue the paths to sustainable energy.

INTECH
open science | open minds

InTech Europe
University Campus STeP Ri
Slavka Krautzeka 83/A
51000 Rijeka, Croatia
Phone: +385 (51) 770 447
Fax: +385 (51) 686 166
www.intechopen.com

InTech China
Unit 405, Office Block, Hotel Equatorial Shanghai
No.65, Yan An Road (West), Shanghai, 200040, China
中国上海市延安西路65号上海国际贵都大饭店办公楼405单元
Phone: +86-21-62489820
Fax: +86-21-62489821

IntechOpen